Angle-resolved photoemission study of $K_{0.3}MoO_3$: direct observation of temperature-dependent Fermi surface across the Peierls transition

2005 J. Phys.: Condens. Matter 17 4935

(http://iopscience.iop.org/0953-8984/17/32/007)

INSTITUTE OF PHYSICS PUBLISHING JOURNAL OF PHYSICS: CONDENSED MATTER

J. Phys.: Condens. Matter **17** (2005) 4935–4940 doi:10.1088/0953-8984/17/32/007

Angle-resolved photoemission study of $K_{0.3}MoO_3$: direct observation of temperature-dependent Fermi surface across the Peierls transition

H Ando[1], T Yokoya[2], K Ishizaka[1], S Tsuda[1], T Kiss[1], S Shin[1,3], T Eguchi[4], M Nohara[4] and H Takagi[4]

[1] Institute for Solid State Physics, University of Tokyo, Kashiwa, Chiba 277-8581, Japan
[2] Japan Synchrotron Radiation Research Institute (JASRI)/Spring-8, Sayo-gun, Hyogo 679-5198, Japan
[3] The Institute of Physics and Chemical Research (RIKEN)/Spring-8, Sayo-gun, Hyogo 679-5148, Japan
[4] Department of Advanced Materials Science, University of Tokyo, Kashiwa, Chiba 277-8581, Japan

Received 21 February 2005, in final form 1 June 2005
Published 29 July 2005
Online at stacks.iop.org/JPhysCM/17/4935

Abstract

The temperature dependence of the low-energy electronic state for a typical quasi-one-dimensional material $K_{0.3}MoO_3$ has been investigated using high-resolution angle-resolved photoemission spectroscopy. We observed well-defined open quasi-one-dimensional Fermi surfaces (FSs) throughout the entire Brillouin zone. The warping of the FSs arising from the finite interchain transfer is also clearly discernible; this seems to be reduced at low temperature. It is indicative of the variation of the nesting condition, from imperfect to nearly perfect, on decreasing the temperature across the Peierls transition.

(Some figures in this article are in colour only in the electronic version)

Molybdenum blue bronze $K_{0.3}MoO_3$ is a typical quasi-one-dimensional (quasi-1D) material, which exhibits a Peierls (metal–insulator) transition at $T_P = 180$ K accompanied by the formation of a charge-density wave (CDW) [1–4]. It has a highly anisotropic crystal structure (centred monoclinic, space group $C2/m$) with 1D MoO_6 octahedral chains along the b direction and their network along the d ($=(1/2)(a+2c)$) direction forming a weakly connected b–d layer which stacks as shown in figures 1(a) and (b) [5]. Reflecting such a crystal structure, $K_{0.3}MoO_3$ shows a strongly anisotropic electrical resistivity, which is the smallest along the b direction (ρ_b:ρ_d:$\rho_{n(\perp b,d)} = 1$:100:1000) [2]. The CDW formation below T_P in this compound has been studied intensively with various experimental techniques. X-ray and neutron scattering studies [6–13] observed the superlattice structure due to the CDW, whose modulation vector is denoted as $Q_{CDW} = (0, q_b, 1/2)$ where q_b varies from $0.724b^*$ at 200 K (fluctuating state)

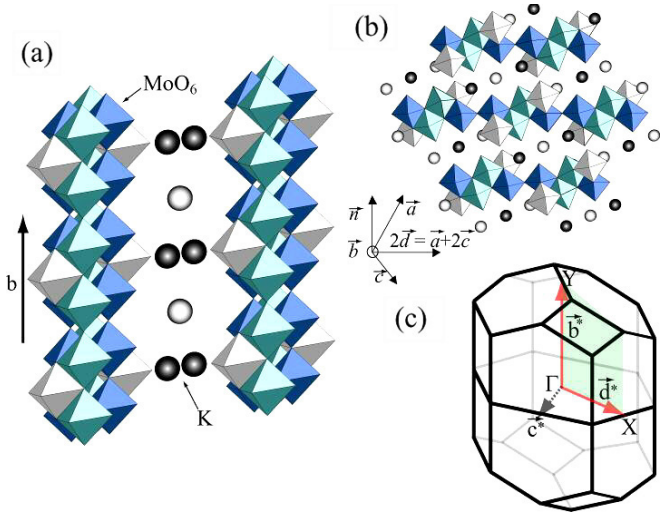

Figure 1. Crystal structure of molybdenum blue bronze $K_{0.3}MoO_3$, showing the infinite chains of MoO_6 octahedra (a) and the cross section of the infinite chains with the a–c plane (b). Note that the chains are connected along the d direction, forming a layer parallel to the b–d plane. (c) The Brillouin zone of $K_{0.3}MoO_3$ for the simple monoclinic structure.

to $0.746b^*$ at 70 K [9]. The resistivity, on the other hand, shows an abrupt increase below T_P, indicating the occurrence of the simultaneous metal–insulator transition, which is characterized by the activation energy of $2\Delta = 60$–80 meV at low temperature (T) [4]. The optical studies also suggest the evolution of the charge gap ($2\Delta = 74$–100 meV) below T_P [14].

Angle-resolved photoemission spectroscopy (ARPES) is a technique that can directly investigate the topology of the Fermi surface (FS), which plays the most important role for driving a CDW transition by the nesting mechanism. To date, several high-resolution ARPES experiments have been performed for $K_{0.3}MoO_3$, focusing on electronic structures near the Fermi level (E_F); these have succeeded in observing detailed band dispersions, the formation of a gap, anomalous spectral function line-shape, etc, including their T-dependence [15–20]. However, since most of these measurements were limited on the high symmetry line Γ Y, the precise topology of the whole FS, which is relevant for investigating its nesting character, still remained to be elucidated.

In this paper, we report on T-dependent high-resolution ARPES studies across T_P at 70 and 200 K to closely investigate the FS topology of $K_{0.3}MoO_3$ in a wide Brillouin zone (BZ) region. We observed the well-defined quasi-1D FSs over a whole BZ with a gentle warping along the d^*-axis. From the T-dependence, we discuss the possible relationships between FS topology, nesting vector, and CDW formation.

Single crystals of $K_{0.3}MoO_3$ (typical size of $\sim 3 \times 1 \times 0.1$ mm^3) were prepared by electrolytic reduction of MoO_3–Na_2MoO_4 mixtures, as described in [21]. ARPES measurements were performed on a spectrometer built using a Scienta SES2002 electron analyser and a GAMMADATA high-flux discharging lamp with a toroidal grating monochromator. The energy and angular resolution using a He Iα (21.218 eV) resonance line were set to $\sim$20 meV and $\pm 0.1^\circ$ (corresponding to 0.0067 Å^{-1}), respectively, to obtain reasonable count rates. Samples were cooled using a flowing liquid He refrigerator with improved thermal shielding. Sample temperature T was measured using a silicon-diode sensor mounted below the samples. The base pressure of the spectrometer was better

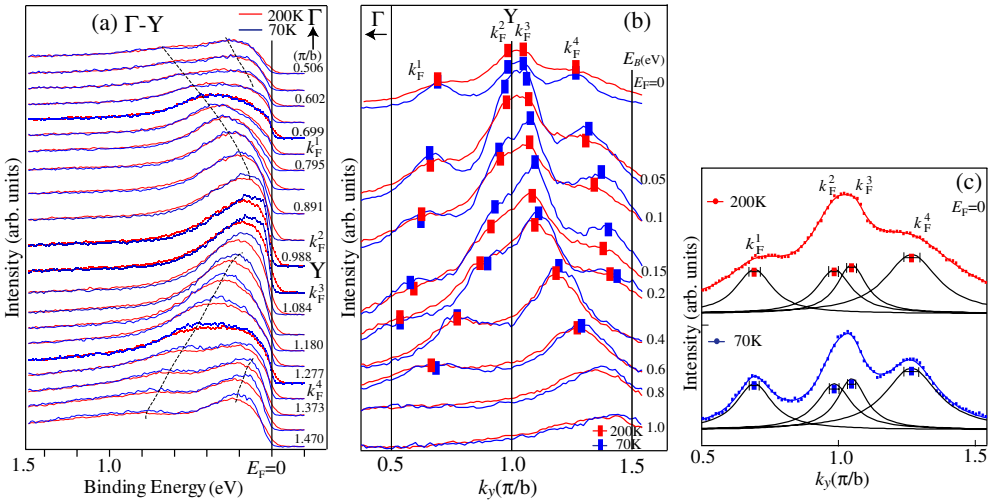

Figure 2. ARPES spectra of $K_{0.3}MoO_3$ at 200 K (red) and 70 K (blue) represented as (a) EDCs and (b) MDCs along the ΓY direction. The broken lines are guides for the eyes, indicating the possible band dispersion. Peak positions determined from Lorentzian fittings are denoted by filled squares. (c) MDCs at E_F (dots) together with the results of Lorentzian analysis (curves).

than 5×10^{-11} Torr. All measurements were carried out on fresh *in situ* cleaved surfaces corresponding to the *b–d* plane ($\bar{2}01$) within 6 h of the cleavings (longer exposure of the cleaved surfaces induced modification of the spectra). The sample orientation was checked by symmetry of ARPES spectra. T-dependent spectral changes were confirmed by cycling T. The Fermi level (E_F) of the samples was referenced to that of a gold film evaporated onto the sample substrate with an accuracy of better than ±1 meV.

Figure 2(a) shows the T-dependence of the energy distribution curves (EDCs) across T_P along the ΓY direction. The EDCs at 200 K (red) and 70 K (blue) are normalized with the integral intensities of the region from 1.0 to 1.5 eV E_B. We find two features at about 0.65 and 0.25 eV E_B in the spectra measured at 0.506 π/b, showing larger and smaller dispersions toward E_F, respectively (indicated with the broken lines). The two features show symmetrical dispersions with respect to the Y point. The Fermi edge cannot be observed in any EDC even at 200 K, where the conductivity is fairly metallic. It is indicative of the non-Fermi liquid-like behaviour possibly attributed to the low dimensionality, CDW fluctuation, or strong electron–phonon coupling, as discussed previously [15–17]. The dispersive features and the anomalous spectral shape are consistent with those reported from previous ARPES studies [15–19]. Compared with results at 200 K, a decrease of intensity at E_F with the energy shift of the leading edge (<20 meV) is observed at 70 K, which arises from the CDW gap opening across T_P.

To determine the energy and momentum (k) positions of these features, we plotted the momentum distribution curves (MDCs) for 200 K (red) and 70 K (blue) as a function of E_B obtained by an energy integration of E_B ± 25 meV, as shown in figure 2(b). For 200 K MDCs, four band dispersions are clearly recognized by following the well-defined peaks for higher E_B regions, namely 0.1–0.2 eV. Near E_F, two dispersive features near Y are located very closely, but they still give shoulders in the MDC. In order to distinguish each component and determine the Fermi momentum (k_F), we fitted each MDC with the least-squares method using four Lorentzian curves, the peak positions of which are indicated with filled squares in

figure 2(b). We also show intensity-enlarged MDCs at E_F (dots) with the four Lorentzians similarly used for the fitting (black lines), and the sum of the Lorentzians (coloured lines) in the upper panel of figure 2(c). From the analysis, four band dispersions crossing E_F at $k_F^1 \sim 0.69$, $k_F^2 \sim 0.98$, $k_F^3 \sim 1.05$, and $k_F^4 \sim 1.27$ (π/b) are clearly discernible. These values of k_F are also in a good accordance with those extrapolated from the high-E_B region. The band dispersions are qualitatively consistent with the band calculation [22, 23], as well as that of the previous ARPES results [15–19]. According to the band calculation, k_F^2 and k_F^4 correspond to the Mo4d–O2p bonding (B) band, while k_F^1 and k_F^3 belong to the anti-bonding (AB) band. Below T_P at 70 K, the MDCs show narrower peaks but the dispersions are nearly the same as that at 200 K. In spite of the loss of intensity due to the gap opening, the peaks are still obvious at E_F (the lower panel of figure 2(c)), enabling us to determine k_F even for 70 K.[5]

To see the FS topology in a wide BZ region, we measured the ARPES spectra along b^*, scanning at every one degree for the direction along d^*, at 200 and 70 K, and plotted the two-dimensional (b^*–d^* plane) map of intensity at E_F which is normalized to the maximum intensity at each T, as shown in figures 3(a) and (b), respectively. The entire map is obtained by the symmetrization of the data at first–second BZ (left-hand side). The high contrast regions (see the colour scale at the bottom of figure 3) at k_Fs correspond to the FSs (the FSs disappear at 70 K due to the CDW gap opening; however, here we call the valence band maximum 'FS' for convenience). The k_Fs estimated from the MDCs previously mentioned are also plotted with filled-circle markers, blue (red) for the AB (B) band, which show good agreement with the pattern of the mapped contrast. For 200 K FS, we observe four open quasi-1D FSs throughout the BZ. We also find that the respective FS obtained in our experiments has a finite curvature (warping). The clearest warping is observed for the B band in the second BZ (k_F^4), depicted with a solid curve (red) as a guide for the eyes. The FS sheets derived from k_F^2 and k_F^3 appear to following the shape of the zone boundary. The warping of the FS indicates a finite interchain transfer along the d-direction (see figure 1(b)), as predicted from the band structure calculations [22, 23]. Focusing on the warping structure for the B band, we recognize that the curvature becomes smaller at 70 K. Previous ARPES studies on $K_{0.3}MoO_3$ [20] showed a T-dependent change in k_Fs along ΓY and correlated it with the T-dependent change in the CDW vector along the chain direction, q_{CDW}^b, reported from neutron scattering studies [10]. It also predicted the shape and T-dependence of the FS using tight-binding calculations. The FS topology and its change observed from the present study agree with the calculated results.

Here, we can make a further step in understanding the nesting character of the FS in $K_{0.3}MoO_3$ by taking advantage of obtaining the experimental T-dependent FS. The CDW modulation vector $Q_{CDW} = (0, q_{CDW}^b, 1/2)$ obtained from the neutron scattering studies [9] is indicated by the arrows in figure 3. It is expected in this compound that the nesting vector connects the FSs formed by the AB band and the B band. From our results at 70 K the b^*-component of the nesting vector determined by k_F^3 and k_F^4 is estimated to be $q_{nest}^b = 0.77(\pm 0.05)b^*$, which corresponds well with the reported value obtained from neutron studies. As for the nesting condition when the warping of the FSs is considered, it is expected to be poor at 200 K. This is because the curvatures for k_F^4 are larger at 200 K than at 70 K, while those for $k_F^{3'}$ (k_F's are the mirror symmetry equivalents of k_Fs) FSs remain similar across the transition. Consequently, the curvatures for these FSs at 70 K seem to become flatter and to nearly coincide. This result clearly indicates that the nesting condition of the FSs varies from imperfect (200 K) to nearly perfect (70 K), as T is lowered across T_P (180 K). Taking account of the x-ray scattering study which observed only diffuse streaks at $T > T_P$ [6], it

[5] Throughout this study, we define k_F as a peak position of the MDC at E_F, which corresponds to the valence band maxima in case of the gapped state.

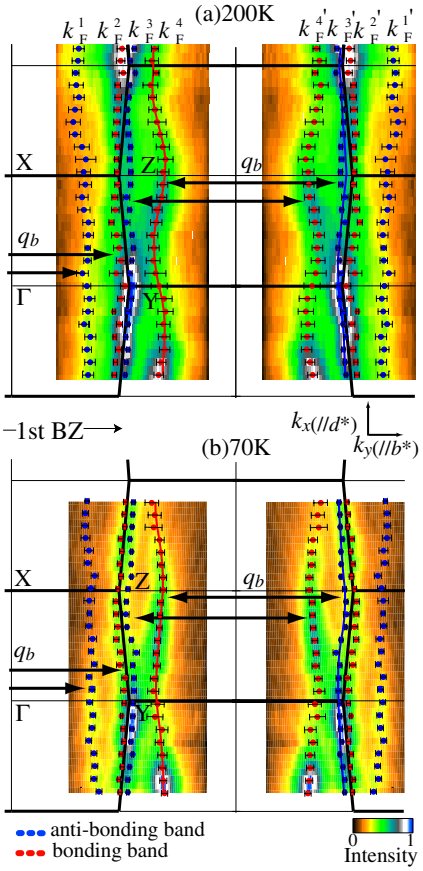

Figure 3. Fermi surface of $K_{0.3}MoO_3$ at 200 K (a) and 70 K (b) plotted as the mapping of intensity at E_F. Peak positions denoted by red (bonding band) and blue (anti-bonding band) filled circles are obtained by fitting the MDCs. Here we also indicate Δk as the measure of the error bar for k_F, which was estimated as the full width at 95% of the respective peak maximum. The arrows represent the b-component of the Q_{CDW} reported from the neutron scattering study [9]. The solid curves (red and blue) are guides for the eyes, indicating the possible curvature of the FSs.

is expected that a nearly perfect nesting condition is required for the static long-range CDW formation in this quasi-1D system. Such an argument of the T-dependent FS topology across the Peierls transition is reported for the first time in $K_{0.3}MoO_3$. The previous ARPES FS mapping result [18] was obtained only at 300 K with ambiguously smeared FS structure, which also failed in resolving k_F^2 and k_F^3 due to the low resolution. Our precise FS study on $K_{0.3}MoO_3$, a typical CDW material appearing in numerous reviews and textbooks, may offer an important clue for understanding the general nature of the 1D system.

In summary, we have succeeded for the first time in obtaining the precise map of quasi-1D FS topology in b^*–d^* plane for a whole BZ region. We observed the warping of the FS, a weak curvature along d^* arising from the small interchain charge transfer, which is slightly modified with lowering temperature. Taking account of the warping, the nesting character of FSs is discussed in comparison with the previously reported diffraction results. Its T-dependence across T_P indicates that a nearly perfect nesting condition is a prerequisite for forming a static CDW.

Acknowledgments

This work was supported by the Ministry of Education, Culture and Science of Japan, and the Japan Society for the Promotion of Science (JSPS). ST and TK are grateful for financial support from a JSPS fellowship.

References

[1] Travaglini G, Wachter P, Marcus J and Schlenker C 1981 *Solid State Commun.* **37** 599
[2] Schlenker C, Filippini C, Marcus J, Dumas J, Pouget J P and Kagoshima S 1983 *J. Physique Coll.* IV **44** C3 1757
[3] Kwok R S, Grüner G and Brown S E 1990 *Phys. Rev. Lett.* **65** 365
[4] Brütting W, Nguyen P H, Rieß W and Paasch G 1995 *Phys. Rev.* B **51** 9533
[5] Graham J and Wadsley A D 1966 *Acta Crystallogr.* **20** 93
[6] Pouget J P, Kagoshima S, Schlenker C and Marcus J 1983 *J. Physique* **44** L-113
[7] Tamegai T, Tsutsumi K, Kagoshima S, Sato M, Tsuji K, Harada J, Sakata M and Nakajima T 1984 *Solid State Commun.* **51** 585
[8] Pouget J P, Noguera C, Moudden A H and Moret R 1985 *J. Physique* **46** 1731
[9] Sato M, Fujishita H, Sato S and Hoshino S 1985 *J. Phys. C: Solid State Phys.* **18** 2603
[10] Fleming R M, Schneemeyer L F and Moncton D E 1985 *Phys. Rev.* B **31** 899
[11] Pouget J P, Girault S, Moudden A H, Hennion B, Escribe-Filippini C and Sato M 1989 *Phys. Scr.* T **25** 58
[12] Girault S, Moudden A H and Pouget J P 1989 *Phys. Rev.* B **39** 4430
[13] Pouget J P, Hennion B, Escribe-Filippini C and Sato M 1991 *Phys. Rev.* B **43** 8421
[14] Schwartz A, Dressel M, Alavi B, Blank A, Dubois S, Grüner G, Gorshunov B P, Volkov A A, Kozlov G V, Thieme S, Degiorgi L and Lévy F 1995 *Phys. Rev.* B **52** 5643
[15] Perfetti L, Mitrovic S, Margaritondo G, Grioni M, Forró L, Degiorgi L and Höchst H 2002 *Phys. Rev.* B **66** 75107
[16] Perfetti L, Mitrovic S and Grioni M 2002 *J. Electron Spectrosc. Relat. Phenom.* **127** 77
[17] Grioni M, Perfetti L and Berger H 2004 *J. Electron Spectrosc. Relat. Phenom.* **137** 417
[18] Gweon G-H, Allen J W, Claessen R, Clack J A, Poirier D M, Benning P J, Olson C G, Ellis W P, Zhang Y-X, Schneemeyer L F, Marcus J and Schlenker C 1996 *J. Phys.: Condens. Matter* **8** 9923
[19] Gweon G-H, Denlinger J D, Allen J W, Claessen R, Olson C G, Höchst H, Marcus J, Schlenker C and Schneemeyer L F 2001 *J. Electron Spectrosc. Relat. Phenom.* **117** 481
[20] Fedorov A V, Brazovskii S A, Muthukumar V N, Johnson P D, Xue J, Duda L-C, Smith K E, McCarroll W H, Greenblatt M and Hulbert S L 2000 *J. Phys.: Condens. Matter* **12** L191
[21] Wold A, Kunnmann W, Arnott R J and Ferretti A 1964 *Inorg. Chem.* **3** 545
[22] Waghmare U V, Kim H, Park I J, Modine N, Maragakis P and Kaxiras E 2001 *Comput. Phys. Commun.* **137** 341
[23] Mozos J-L, Ordejón P and Canadell E 2002 *Phys. Rev.* B **65** 233105